

Dielectric properties and microstructures of Ta-doped BaTiO₃–(Bi_{0.5}Na_{0.5})TiO₃ ceramics for X9R applications

Zhengbo Shen¹ · Xiaohui Wang¹ · Longtu Li¹

Received: 13 August 2016 / Accepted: 31 October 2016 / Published online: 7 November 2016
© Springer Science+Business Media New York 2016

Abstract Ta-doped 0.90BaTiO₃–0.10(Bi_{0.5}Na_{0.5})TiO₃ ceramics were successfully prepared by conventional solid-state reaction method and studied to satisfy super-broad temperature stability. The effects of Ta₂O₅ doping on the dielectric properties and microstructures were thoroughly investigated. Ta plays an important role in the formation of core–shell structure because of chemical inhomogeneity, which gives rise to the weak temperature dependence of dielectric properties. The samples with the addition of 1.5 mol% Ta₂O₅ satisfy the X9R specification, exhibiting an optimum dielectric behavior of $\epsilon_r \sim 2100$, $\tan\delta \sim 1.6\%$ at room temperature, which is a promising candidate material for X9R MLCC applications.

1 Introduction

Multilayer ceramic capacitors (MLCCs) are particularly important electronic components used in almost every area of electronics. While in some harsh conditions, such as oil drilling, aerospace and automotive environment, the electronic devices must withstand high temperature nearly at 200 °C [1, 2]. Therefore, X7R (–55 to 125 °C, $\Delta C/C_{25\text{ °C}} \leq \pm 15\%$) and X8R-type (–55 to 150 °C, $\Delta C/C_{25\text{ °C}} \leq \pm 15\%$) MLCCs of the Electronic Industries Association (EIA) standards cannot fulfill the requirement because their ceiling temperatures are 125 and 150 °C, respectively [3–5]. The increasing current demand drives

the study of broad temperature stable materials used in higher temperature electronic components. Nowadays, it is necessary to exploit systems which can satisfy EIA-X9R specifications (–55 to 200 °C, $\Delta C/C_{25\text{ °C}} \leq \pm 15\%$).

It is universally known that compositions of most ceramic dielectrics are based on the barium titanate (BaTiO₃) materials. However, pure BaTiO₃ (BT) ceramics do not meet the temperature stability requirements ($\Delta C/C_{25\text{ °C}} \leq \pm 15\%$) due to the dramatic variation of permittivity above the Curie temperature ($T_c \sim 130\text{ °C}$), obeying Curie–Weiss law. For MLCC formulation, BT can be either chemically or physically modified to exhibit the required temperature-stable dielectric behavior [4]. A range of lead-free BT-based systems have been developed in the search for new high temperature dielectric materials, such as compositions in the solid solution series BaTiO₃–Ba(Zn_{0.5}Ti_{0.5})O₃ [6–8]; BaTiO₃–LiTaO₃ [9]; BaTiO₃–Bi(Mg_{0.5}Zr_{0.5})O₃ [10]; BaTiO₃–(Bi_{0.5}Na_{0.5})TiO₃ [11–18] and so on. BaTiO₃–(Bi_{0.5}Na_{0.5})TiO₃ (BT–BNT) system exhibits outstanding performance for X9R MLCCs application among these candidates. To achieve X9R specifications, a key technical requirement is to develop a fine-grained core–shell microstructure with a controlled dopant gradient within the BT–BNT grains. Researchers find that proper dopants, such as Nb, Co, play important roles to maintain the core–shell structure in the BT–BNT system [11–14, 16, 18–20]. However, there are limited investigations on the effect of Ta in the BT–BNT system.

In the present work, 0.90BaTiO₃–0.10(Bi_{0.5}Na_{0.5})TiO₃ (9010BTBNT) ceramics modified by Ta₂O₅ with high permittivity meeting X9R specification were prepared by conventional solid-state reaction method. TEM observations show that well developed core–shell structure exists in almost every grain. The effects of Ta₂O₅ on the dielectric properties and microstructures of the Ta₂O₅–

✉ Xiaohui Wang
wxh@mail.tsinghua.edu.cn

¹ State Key Laboratory of New Ceramics and Fine Processing, School of Materials Science and Engineering, Tsinghua University, Beijing 100084, People's Republic of China

doped 9010BTBNT ceramics were also thoroughly investigated.

2 Experimental procedures

The experimental procedure of fabricating 9010BTBNT ceramics is depicted in Fig. 1. $(\text{Bi}_{0.5}\text{Na}_{0.5})\text{TiO}_3$ (BNT) powders were synthesized by conventional solid-state reaction method, by using Bi_2O_3 (Analytical Reagent, Sinopharm Chemical Reagent Co., Ltd), Na_2CO_3 (Analytical Reagent, Sinopharm Chemical Reagent Co., Ltd), and TiO_2 (Analytical Reagent, Aladdin Chemistry Co., Ltd) as raw materials. Na_2CO_3 was firstly dried in a vacuum drying oven at 80°C and mixed these oxides according to stoichiometric ratio by ball milling using ethyl alcohol as medium for 24 h. Then, the mixed powder was dried and calcined at 900°C for 3 h to obtain a perovskite phase of BNT. Perovskite solid solution 9010BTBNT was prepared by mixing commercial BT (Electronic Grade, Guoci Dongying) powders with average size of 50 nm and BNT powders derived in advance. BT and BNT powders were mixed at a mole ratio of 9:1 by ball milling using ethyl alcohol as medium for 24 h. The mixture was then dried and calcined at 1000°C for 3 h to form the pure perovskite structure. Subsequently, various amounts reagent-grade Ta_2O_5 (i.e., 1.0, 1.5, 2.0, 2.5 mol%) were added into the 9010BTBNT powders by ball-milling using the deionized water as medium for 24 h. After drying, the powders were mixed with PVB binder and pressed into disks with 10 mm in diameter and about 1 mm in thickness. Finally, the pellets were sintered at 1200°C for 2 h in air atmosphere (Table 1).

The phase structures of powders and ceramics were detected by X-ray diffraction meter (XRD, D8 Advance, Bruker Inc., Germany, $\lambda = 1.54178 \text{ \AA}$) with a $\text{Cu K}\alpha$ radiation in the 2θ range from 10° to 90° with a scanning

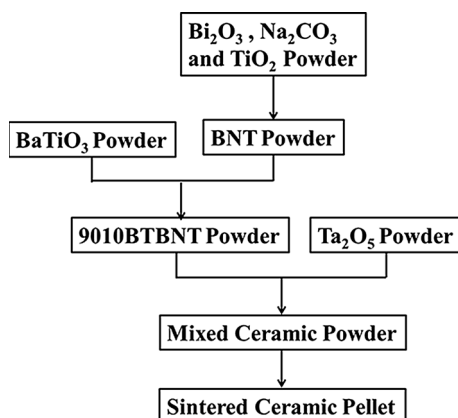


Fig. 1 Flow chart for the fabrication of the 9010BTBNT ceramics (Color online)

Table 1 Dielectric and electrical properties at room temperature for the samples

Content of Ta_2O_5 (mol%)	ϵ_r	$\tan\delta$	Resistivity ($10^{12} \Omega \text{ cm}$)
1.0	1808	0.026	0.72
1.5	2121	0.016	1.87
2.0	1580	0.016	1.83
2.5	1384	0.015	1.25

speed of $6^\circ/\text{min}$ in the normal routine. The microstructures of the specimens were observed by scanning electron microscopy (SEM; MERLIN VP Compact, Carl Zeiss, Oberkochen, Germany) with an accelerating voltage of 10 kV and transmission electron microscopy (TEM, JEOL-2010F, Tokyo, Japan) equipped with energy dispersive spectroscopy (EDS). For electric measurements, silver paste electrodes were first printed onto the sample, which was fired at 550°C for 30 min. Dielectric properties of the samples were measured from -100 to 250°C (heating rate $3^\circ\text{C}/\text{min}$) using an impedance analyzer (Model E4980A, Agilent Technologies, Santa Clara, California, United States) at a frequency of 1 kHz and oscillation level of 1.0 V. Additionally, the insulation resistance was measured with a pA meter (Model HP4140B, Hewlett-Packard Company, Santa Clara, California, United States).

3 Results and discussion

Figure 2 shows the XRD patterns of the 9010BTBNT- x mol% Ta_2O_5 ceramics with $1.0 \leq x \leq 2.5$ sintered at 1200°C for 2 h. The main crystal phases of all the samples could be indexed by BaTiO_3 crystal structures. All the samples display a desired perovskite structure with trace amounts of Ti-rich second phases, identified as $\text{Ba}_6\text{Ti}_{17}\text{O}_{40}$. However, in addition to the $\text{Ba}_6\text{Ti}_{17}\text{O}_{40}$ phase, another second-phase

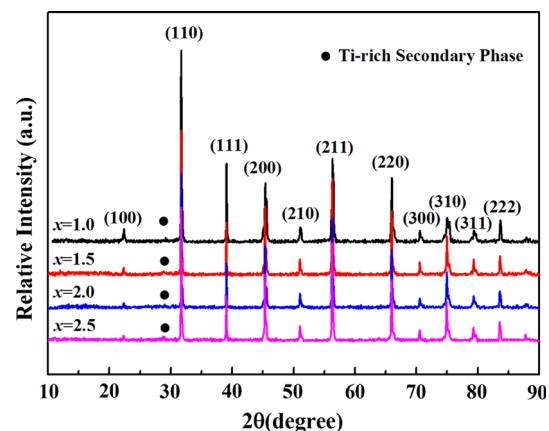
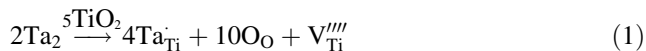


Fig. 2 XRD patterns of 9010BTBNT ceramic samples with various amount of Ta_2O_5 (Color online)

$\text{Ba}_6\text{Ti}_{14}\text{Nb}_2\text{O}_{39}$ was found in Nb-doped 9010BTBNT as reported in the literatures [14, 21]. This result implied that Ta^{5+} completely diffused into the lattices and the solubility of Ta^{5+} in 9010BTBNT system is larger than Nb^{5+} [14]. As a B-site substitute, Ta^{5+} (0.064 nm) exclusively occupies Ti-site and acts as a donor due to the size of the ionic diameter. This leads to the formation of cation vacancies to neutralize the electrical system as interpreted in the following Eq. (1):



It is suggested that higher concentration of Ti-site vacancies result easily in the instability of the host structure which precipitates Ti-rich second phase [11, 22].

The surface morphologies of the Ta_2O_5 -doped 9010BTBNT ceramics were shown in Fig. 3, revealing grain and grain boundary microstructure. All the samples were highly densified with homogeneous fine grained microstructures. The microstructural evolution of the sintered 9010BTBNT ceramics was further investigated with TEM studies. Figure 4 presents the TEM image of the 1.5 mol% Ta_2O_5 -doped 9010BTBNT ceramics. TEM observations reveal a core-shell microstructure within each grain. Well-developed domain structures, the characteristic features of ferroelectric phases [23, 24], are observed only in the core region of grains. The existence of domain structures in the core regions indicate that the true structure of 9010BTBNT is tetragonal instead of cubic, while the shell is closer to cubic symmetry.



Fig. 4 TEM micrographs of 9010BTBNT ceramic samples doped with 1.5 mol% Ta_2O_5 (Color online)

Figure 5 shows the TEM image of the typical ceramic grain in 1.5 mol% Ta_2O_5 -doped 9010BTBNT ceramics and EDS analysis results of the core-shell structure of this grain, which was carried out along AB line scanning and map scanning of the whole grain. From the grain boundary to the grain core, the content of Ta decreases gradually to a very low level after a certain distance, exhibiting a form of “U” curve along AB line as illustrated in Fig. 5b. The results were further confirmed by the EDS mapping analysis within the whole grain as shown in Fig. 5c–h, delineating the distributions of all elements. Figure 5h indicates that the whole grain is composed of two kinds of regions: Ta-rich region and Ta-poor region, corresponding to the

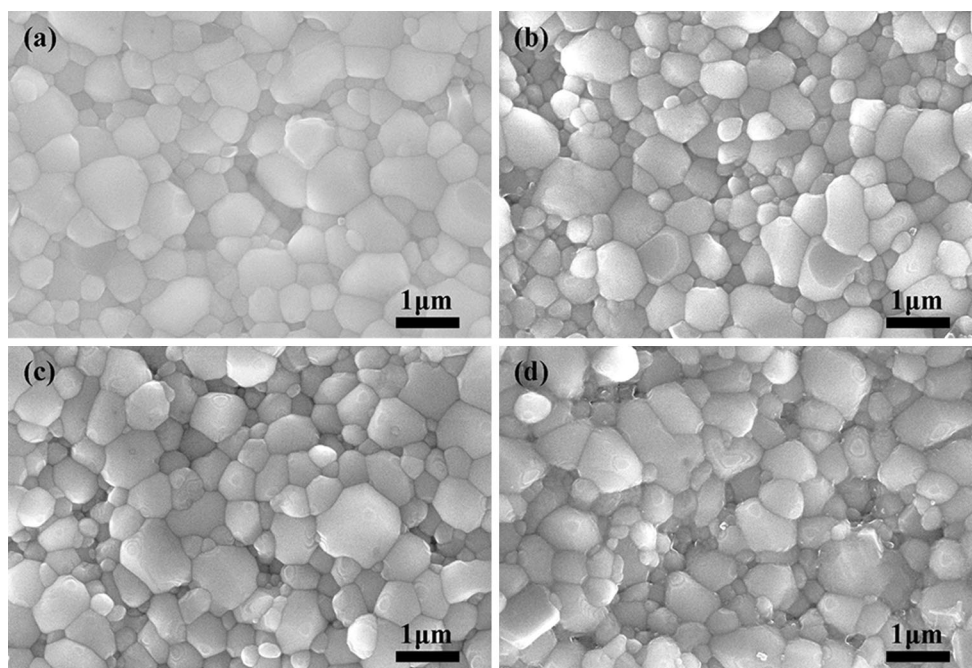
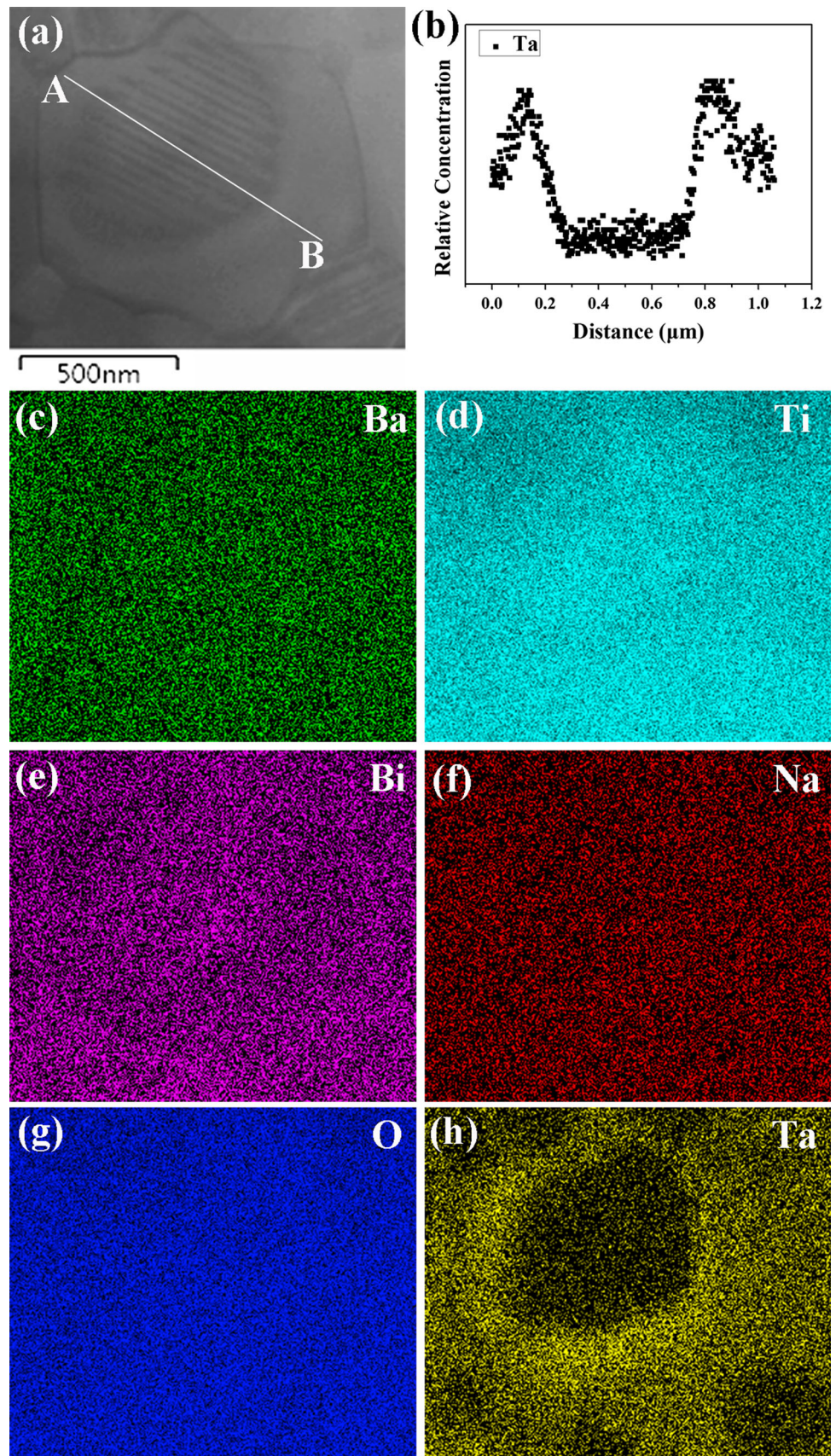


Fig. 3 SEM graphs of 9010BTBNT ceramic samples with various amount of Ta_2O_5 : **a** $\text{Ta}_2\text{O}_5 = 1.0$ mol%; **b** $\text{Ta}_2\text{O}_5 = 1.5$ mol%; **c** $\text{Ta}_2\text{O}_5 = 2.0$ mol%; **d** $\text{Ta}_2\text{O}_5 = 2.5$ mol% (Color online)

Fig. 5 TEM images of core-shell structure **(a)** and EDS analysis of the 9010BTBNT ceramic samples doped with 1.5 mol% Ta₂O₅. **b** Line profiles of Ta distribution along the *straight line AB* through the grain; mapping results of elements distribution: **c** Ba; **d** Ti; **e** Bi; **f** Na; **g** O; **h** Ta (Color online)



shell and core respectively. However, other elements, namely Ba, Ti, Bi, Na, O, as delineated in Fig. 5c–g, are almost homogeneously distributed in the whole grain. It is concluded that Ta mainly dissolves into the shell region to form the solid solution, while the core region consist of almost pure 9010BTBNT. The results suggest that Ta plays a crucial important role in the formation of core–shell structure, which is similar to that of Nb in the same system [21].

It has been reported that larger ions substitution of Ti^{4+} ions in the oxygen octahedra could modify the polarization of BT-based materials effectively [16, 25]. As a donor, Ta^{5+} enters Ti-site shielded hermetically by the large O^{2-} ions, then centrally located in the oxygen octahedra and got stuck. The polarization in the BT–BNT system mainly originates from the Ti^{4+} ions deviating from the central region of the oxygen octahedral. The deviation would be prevented and cause changing in polarization due to the slightly larger size of Ta^{5+} . Additionally, the octahedra would be inflated due to the incorporation of larger Ta^{5+} ions, which probably altered the adjacent octahedra and thus inhibited the formation of ferroelectric domains. It suggests that the tetragonality decreases and the formation of the ferroelectric domains is suppressed in the Ta-rich parts just as shown in the TEM images.

Figure 6 demonstrates the temperature dependence of dielectric constant, loss tangent and temperature coefficient of capacitance (TCC = $\Delta C/C_{25\text{ }^\circ\text{C}}$) curves for 9010BTBNT samples with various amount of Ta_2O_5 measured at a frequency of 1 kHz over the temperature range from -100 to 250 °C. The curves of temperature dependence of dielectric constant become flatten when Ta_2O_5 was added to 9010BTBNT, which should be attributed to the formation of core–shell structure. The dielectric peak at low temperature corresponds to the shell parts, while the high temperature one

corresponds to the core regions. With the increase of Ta_2O_5 , the low temperature dielectric peak rises while the high temperature peak slightly decreases. This is because more amount of Ta dissolves into the 9010BTBNT, the shell regions broaden and core parts shrink. In addition, the transition temperature T_m , corresponding to the maximum permittivity at high temperature, decreases slightly with increasing the concentration of Ta. According to Datta' study [26], the high transition temperature of BTBNT solid solutions derives from the shortening of the Ti–O bonds. Therefore, the decrease of T_m in Ta-doped BTBNT ceramics should be ascribed to the weakening of Ti–O bonds caused by Ti vacancies when Ta was incorporated into 9010BTBNT.

Temperature-capacitance characteristics are remarkably improved especially at low temperature with the incorporation of Ta_2O_5 , as manifested in Fig. 6b. It can be seen from TCC curves that variation ratio of capacitance shifts slightly to a higher place at low temperature end, while at high temperature, the permittivity peak is suppressed with increasing dopants and the curves shift down gradually. Owing to the formation of core–shell structure, the dramatical variation of permittivity over T_c point is suppressed distinctly as the addition of Ta_2O_5 . Consequently, broad and diffused phase transition takes place, thus resulting in weak temperature dependence over a relatively wide temperature range. It was found that Ta_2O_5 dopant improved TCC performance more efficiently than Nb_2O_5 dopant in the 9010BTBNT ceramics [14, 21]. The samples doped with 1.0 mol% Ta_2O_5 do not satisfy EIA X9R specifications depicted by a dash box as shown in Fig. 6b, while other compositions all fulfill. The samples doped more amount of Ta_2O_5 maintain $\text{TCC} \leq \pm 15\%$ over the measuring temperature range from -100 to 250 °C.

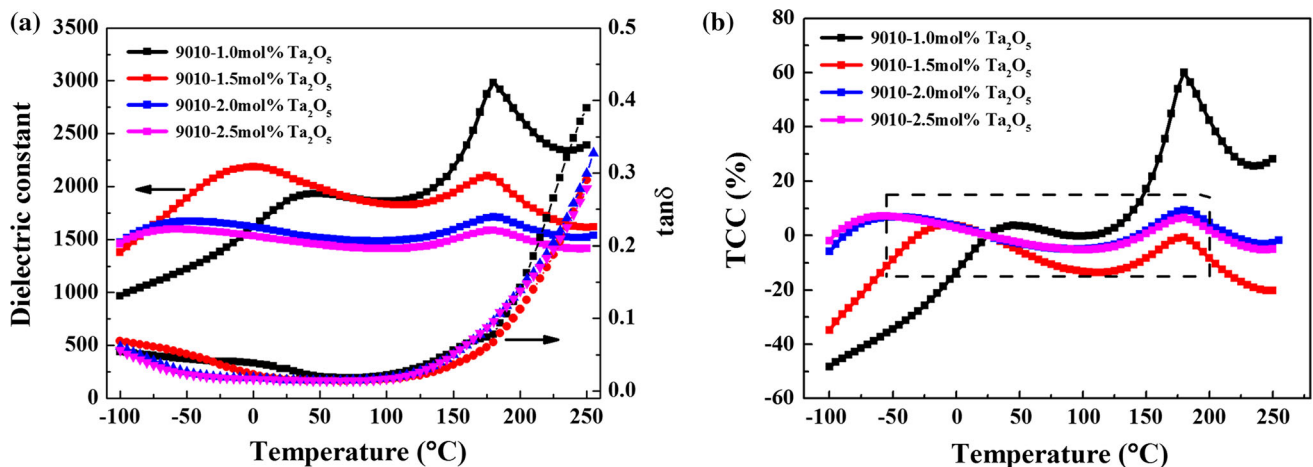


Fig. 6 a Temperature dependence of dielectric constant and loss tangent for 9010BTBNT samples with various amount of Nb_2O_5 . b Temperature coefficient of capacitance (TCC = $\Delta C/C_{25\text{ }^\circ\text{C}}$) curves

for 9010BTBNT samples with various amount of Nb_2O_5 . The dashed box in b shows the X9R specifications (Color online)

4 Conclusions

Ta-doped 9010BTBNT ceramics for X9R MLCCs application have been successfully prepared by conventional solid-state reaction method. The results of TEM and EDS indicated that core–shell structures in this research mainly originated from the inhomogenous distribution of Ta. With the addition of Ta₂O₅, the temperature dependence of the samples was improved and the sample doped more amount of Ta₂O₅ could maintain TCC $\leq \pm 15\%$ over the measuring temperature range (from -100 to 250 °C). The 1.5 mol% Ta₂O₅-doped specimens not only met X9R specifications but also exhibited outstanding performance with a permittivity of 2121, a dissipation factor of 1.6% and electrical resistivity of $1.87 \times 10^{12} \Omega \text{ cm}$ at room temperature at the frequency of 1 kHz. High permittivity, low dielectric loss and weak temperature dependence were obtained concurrently, which ensure the X9R applications of this material.

Acknowledgements The work was supported by Ministry of Sciences and Technology of China through National Basic Research Program of China (973 Program 2015CB654604), National Natural Science Foundation of China for Creative Research Groups (Grant No. 51221291), National Natural Science Foundation of China (Grant No. 51272123), and also supported by CBMI Construction Co., Ltd. Thanks Beijing National Center for Electron Microscopy for the observation of TEM.

References

- M.R. Werner, W.R. Fahrner, *IEEE Trans. Ind. Electron.* **48**, 249 (2001)
- R.W. Johnson, J.L. Evans, P. Jacobsen, J.R. Thompson, M. Christopher, *IEEE Trans. Electron. Packag. Manuf.* **27**, 164 (2004)
- S.F. Wang, G.O. Dayton, *J. Am. Ceram. Soc.* **82**, 2677 (1999)
- W.H. Lee, C.Y. Su, *J. Am. Ceram. Soc.* **90**, 3345 (2007)
- G. Yao, X. Wang, H. Gong, H. Wen, L. Li, *Jpn. J. Appl. Phys.* **50**, 1502 (2011)
- J.B. Lim, S. Zhang, T.R. Shrout, *Electron. Mater. Lett.* **7**, 71 (2011)
- T. Wang, H. Hao, M. Liu et al., *J. Am. Ceram. Soc.* **98**, 690 (2015)
- N. Raengthon, H.J. Brown-Shaklee, G.L. Brennecka, D.P. Cann, *J. Mater. Sci.* **48**, 2245 (2013)
- S.F. Wang, J.H. Li, Y.F. Hsu, Y.C. Wu, Y.C. Lai, M.H. Chen, *J. Eur. Ceram. Soc.* **33**, 1793 (2013)
- A. Zeb, S.J. Milne, *J. Eur. Ceram. Soc.* **34**, 3159 (2014)
- Y. Zhang, S. Gao, B. Zhang, *J. Mater. Sci. Mater. Electron.* **26**, 2709 (2015)
- N. Zhang, L. Li, J. Chen, J. Yu, *Mater. Lett.* **138**, 228 (2015)
- N. Zhang, L. Li, J. Chen, Y. Liu, J. Yu, *Ceram. Int.* **41**, 4805 (2015)
- S.F. Wang, Y.F. Hsu, Y.W. Hung, Y.X. Liu, *Appl. Sci.* **5**, 1221 (2015)
- L. Li, M. Wang, Y. Liu, J. Chen, N. Zhang, *Ceram. Int.* **40**, 1105 (2014)
- L. Li, D. Guo, W. Xia et al., *J. Am. Ceram. Soc.* **95**, 2107 (2012)
- Y. Guofeng, W. Xiaohui, W. Yunyi, L. Longtu, *J. Am. Ceram. Soc.* **95**, 614 (2012)
- Y. Sun, H. Liu, H. Hao, L. Zhang, S. Zhang, *Ceram. Int.* **41**, 931 (2015)
- L. Li, J. Chen, N. Zhang, Y. Liu, J. Yu, *J. Mater. Sci. Mater. Electron.* **26**, 84 (2015)
- Y. Guofeng, W. Xiaohui, Z. Yichi, S. Zhengbo, L. Longtu, *J. Am. Ceram. Soc.* **95**, 3525 (2012)
- Z.B. Shen, X.H. Wang, D.S. Song, L.T. Li, *Adv. Appl. Ceram.* **115**(7), 435–442 (2016)
- D. Hennings, G. Rosenstein, *J. Am. Ceram. Soc.* **67**, 249 (1984)
- D. Viehland, S.J. Jang, L.E. Cross, M. Wuttig, *J. Appl. Phys.* **68**, 2916 (1990)
- H. Ogihara, C.A. Randall, S. Trolier-McKinstry, *J. Am. Ceram. Soc.* **92**, 110 (2009)
- N. Hirose, J. Skakle, A. West, *J. Electroceram.* **3**, 233 (1999)
- K. Datta, K. Roleder, P.A. Thomas, *J. Appl. Phys.* **106**, 123512 (2009)